

Supplementary Materials for

Evidence of link between quorum sensing and sugar metabolism in *Escherichia coli* revealed via cocrystal structures of LsrK and HPr

Jung-Hye Ha, Pricila Hauk, Kun Cho, Yumi Eo, Xiaochu Ma, Kristina Stephens, Soyoung Cha, Migyeong Jeong, Jeong-Yong Suh, Herman O. Sintim, William E. Bentley, Kyoung-Seok Ryu

Published 1 June 2018, *Sci. Adv.* **4**, eaar7063 (2018)
DOI: 10.1126/sciadv.aar7063

This PDF file includes:

- fig. S1. Identification of copurified protein with LsrK.
- fig. S2. SEC-MALS analysis of the purified LsrK/HPr protein complex.
- fig. S3. Electron density maps in the region of the bound HPr, ATP, and ADP.
- fig. S4. Monitoring the stability of the synthesized p-¹⁵NHPr using HSQC experiment.
- table S1. X-ray data collection and refinement statistics.
- table S2. Strains and plasmids used for Miller assay.
- table S3. Primer sequences for the in vivo studies of the wild-type and mutant HPr proteins.

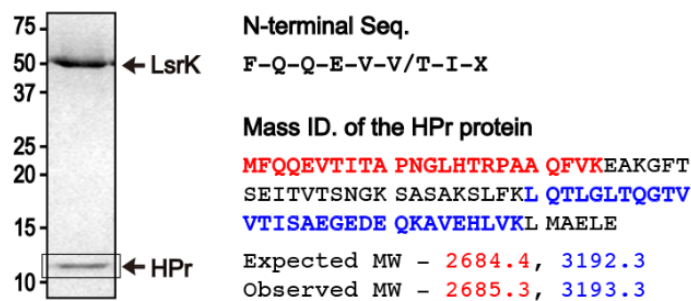


fig. S1. Identification of copurified protein with LsrK. SDS-PAGE analysis of LsrK protein crystal shows the presence of an additional protein band (boxed region in left panel). (i) N-terminal sequencing using Edman degradation and (ii) mass identification after in-gel trypsin-digestion validated that the copurified protein with the LsrK was *E. coli* HPr protein.

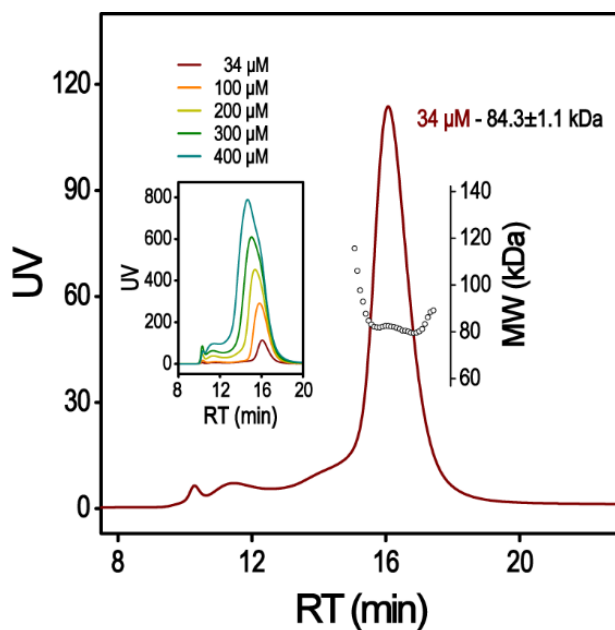


fig. S2. SEC-MALS analysis of the purified LsrK/HPr protein complex. The LsrK/HPr protein complex forms a dimer at elevated concentration. However, the LsrK/HPr protein exists as a monomeric one-to-one complex at low concentrations that are biologically more realistic. SEC-MALS analysis of samples at lower concentration of (1 mg/ml, 14.7 μM) yielded MW (63.9 ± 1.9 kDa) that is more close to the MW of the 'monomeric' LsrK/HPr complex (not shown).

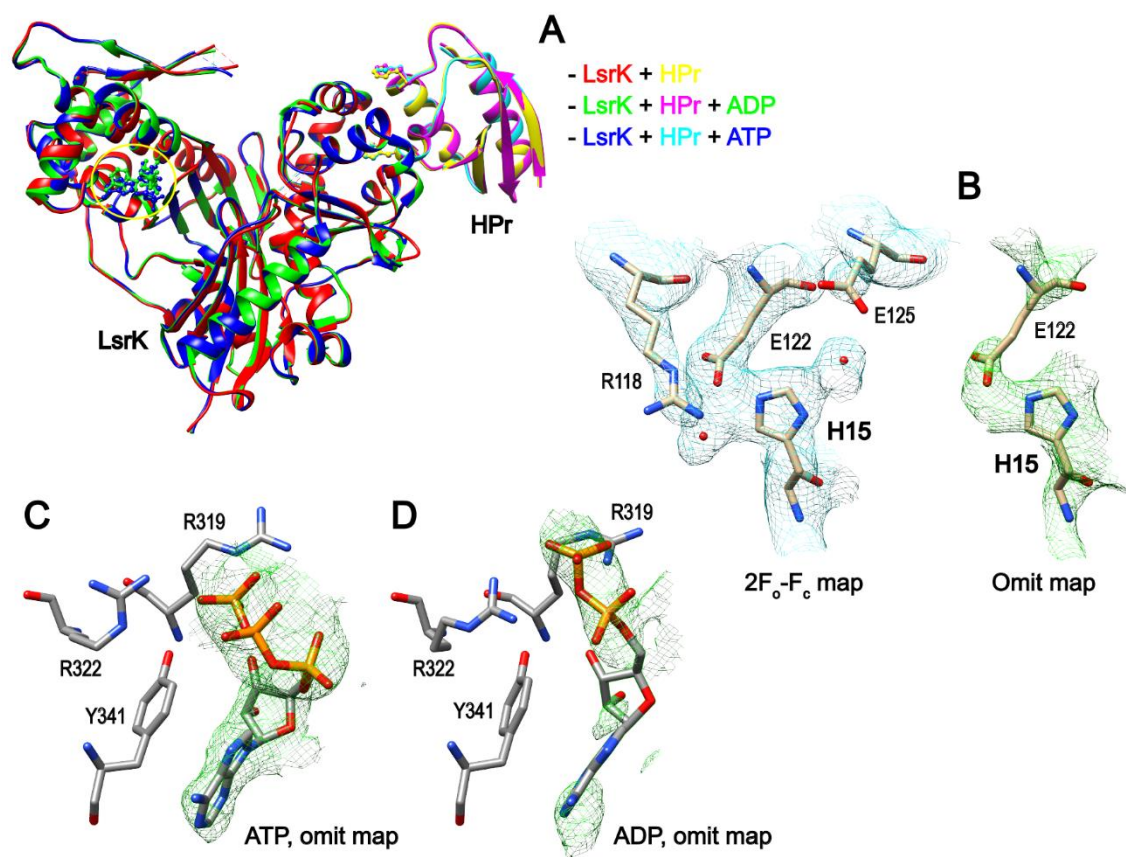


fig. S3. Electron density maps in the region of the bound HPr, ATP, and ADP. (A) The structural overlay of the ^{His}LsrK/HPr, ^{His}LsrK/HPr/ADP, and ^{His}LsrK/HPr/ATP proteins shows that their overall structures are almost identical. (B) The 2F_o-F_c map of the ^{His}LsrK/HPr/ATP complex contoured at 1.0σ (left panel) is shown for the region of the HPr-H15 residue. The simulated annealing (SA) omit map (0.5σ) was calculated for the HPr-H15 and LsrK-E122 residues (right panel). The less clear map in the region of the HPr-H15 and LsrK-E122 shows that the H15 residue likely has motional flexibility. The SA omit maps (0.5σ) show that the occupancy of the ADP molecule in the ^{His}LsrK/HPr/ADP complex (D) was much less than that of the ATP in the ^{His}LsrK/HPr/ATP complex (C).

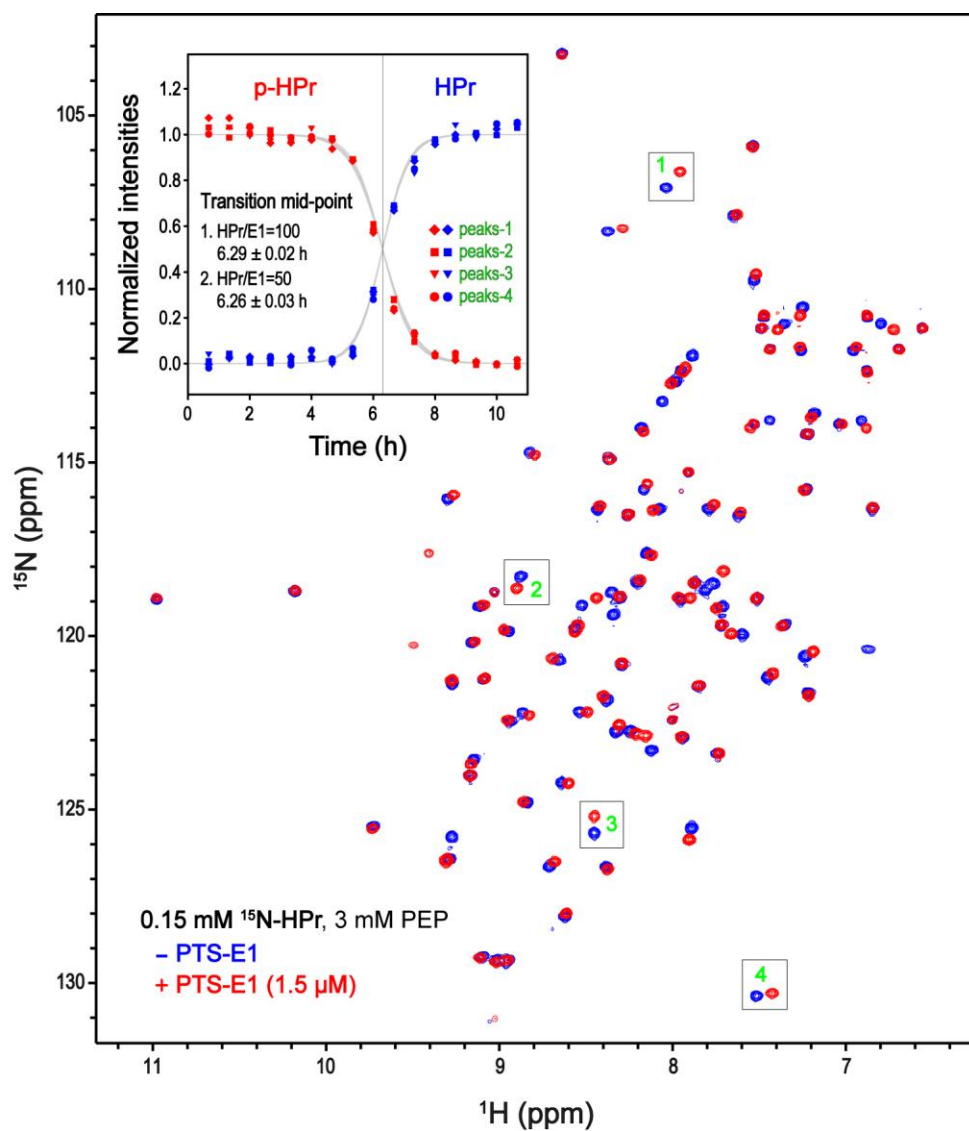


fig. S4. Monitoring the stability of the synthesized p- ^{15}N HPr using HSQC experiment. The incubation of the ^{15}N HPr (0.15 mM) with the EI (1.5 μM) in the presence of 3.0 mM PEP resulted in the complete phosphorylation of the ^{15}N HPr. The one-fourth amount of the EI was also sufficient for the complete phosphorylation (now shown). The synthesized p-HPr was maintained up to 5 h after the initiation of the EI reaction (inset). The presence of twice amount of the EI in the reaction mixture did not notably decrease the life-time of the p- ^{15}N HPr, which indicated that non-productive consumption of PEP by the EI was negligible and the life-time was mainly dependent on the initial concentration of PEP.

table S1. X-ray data collection and refinement statistics.

	HisLsrK/HPr SeMet	HisLsrK/HPr	HisLsrK/HPr/ADP	HisLsrK/HPr/ATP
Resolution (Å)	50.0-3.2 (3.31-3.20)	50.0-3.0 (3.11-3.00)	50.0-2.7 (2.80-2.70)	50.0-2.9 (2.80-2.70)
Space group	P3 ₂ 21	P3 ₂ 21	P3 ₂ 21	P3 ₂ 21
Unit-cell parameters (a, b, c, α, β, γ)	101.26, 101.26, 344.76, 90, 90, 120	101.16, 103.34, 344.32, 90, 90, 120	101.25, 101.25, 344.15, 90, 90, 120	101.02, 101.02, 344.45, 90, 90, 120
Measured reflections	198,323	405,478	387,461	451,089
Unique reflections (#)	34,461	41,484	55,517	55,279
Number of molecules in AU	2	2	2	2
Redundancy	5.8 (4.5)	9.8 (6.1)	7.0 (3.5)	8.2 (4.2)
R _{merge} (%)	9.1 (37.1)	6.2 (39.7)	5.8 (37.8)	6.2 (37.6)
Mean I/Iσ	26.0 (3.5)	22.2 (2.0)	25.9 (2.6)	25.2 (3.0)
Completeness (%)	98.5 (98.3)	98.3 (96.8)	96.9 (94.4)	96.7 (94.3)
R _{cryst} /R _{free}		0.199/0.239	0.214/0.255	0.215/0.231
RMSD bond length (Å)		0.005	0.005	0.004
RMSD bond angle (°)		0.973	0.978	0.841
Ramachandran plot				
Favored (%)		90.0	95.8	96.5
Outliers (%)		0.18	0.18	0.18
Poor rotamers		0.7	0.8	0.8
Molprobtity overall score		1.68	1.69	1.45
Average B factor (Å ²)				
Chain A		31.92	25.58	41.52
Chain B		31.53	24.18	40.37
Chain C				
Chain D				
Water		39.29	32.24	42.07
Ligand		-	28.06	41.11
PDB deposit		5YA0	5YA1	5YA2

table S2. Strains and plasmids used for Miller assay.

Strain or plasmid	Relevant genotype and property	Source or reference
<i>E. coli</i> strains		
DH5 α	Used for cloning	New England labs
ZK126	W3110 $\Delta lacU169$ <i>tna-2</i>	(45)
LW7	W3110 $\Delta lacU169$ <i>tna-2</i> $\Delta luxS::Kan$	(10)
PH01	W3110 $\Delta lacU169$ <i>tna-2</i> $\Delta ptsH::Cm$	This study
PH02	W3110 $\Delta lacU169$ <i>tna-2</i> $\Delta luxS::Kan$ $\Delta ptsH::Cm$	This study
Plasmids		
pSkunk	p15a origin, f1 origin, AadA streptomycin/spectomycin resistance, and <i>tac</i> promoter	(47)
pLW11	pFZY1 derivative, containing <i>lsrACDBFG</i> promoter region, Ap ^r	(10)

table S3. Primer sequences for the in vivo studies of the wild-type and mutant HPr proteins.

Knock-out primers
<i>ptsHdel-F</i> ACCGCCAGGCTAGACTTTAGTTCACACAACACTAAACCTATAAGTTGGGAAATACAgtgtaggctggagctgcttc
<i>ptsHdel-R</i> GCCTGAAATCATAACCCTACCTTACTTGTGACTGATTTTAAAAGAACCCGGGAAAcatatgaatatcctccttag
<i>ptsHout-F</i> GATGCGCGAAATTAATCGTTACAGGAAAAGCC
<i>ptsHout-R</i> CTCCTCATCTTCGAGCAGCATAATATGCCCTTC
Cloning primers
<i>ptsH-BamHI</i> tacgcggatccATGTTCCAGCAAGAAGTTACCATTACCGCTCC
<i>ptsH-SpeI</i> agtctagactagtTTACTCGAGTTCCGCCATCAGTTTAACCG